

# TIME DOMAIN SPHERICAL HARMONIC ANALYSIS FOR ADAPTIVE NOISE CANCELLATION OVER A SPATIAL REGION

Huiyuan Sun, Thushara D. Abhayapala, Prasanga N. Samarasinghe

Research School of Engineering, The Australian National University, Canberra ACT 0200, Australia  
 {huiyuan.sun, thushara.abhayapala, prasanga.samarasinghe}@anu.edu.au

## ABSTRACT

Active Noise Cancellation (ANC) is a well researched topic for minimizing unwanted acoustic noise, and spatial ANC is a recently introduced concept that focuses on continuous spatial regions. Adaptive filter designing for spatial ANC is often based on frequency-domain spherical harmonic decomposition method, which has a major limitation due to the increased system latency. In this paper, we develop a time-domain spherical harmonic based signal decomposition method and use it to develop two time-space domain feed-forward adaptive filters for spatial ANC. Through simulations we show that the proposed methods can achieve higher noise reduction performance over the control region with microphones located on the surface of the region compared to the conventional time-domain adaptive filter.

**Index Terms**— Active noise control, Adaptive filter, Space domain signal processing, Spherical harmonic

## 1. INTRODUCTION

Active noise cancellation (ANC) aims to cancel unwanted noise by producing a secondary sound field [1]. ANC over space is often achieved by multi-channel system with multiple microphones and loudspeakers [2], [3]. Applications of this technique include noise cancellation in cars [4], [5] and in other enclosures [6]. As noises are often time-varying, ANC systems are made to be adaptive both in time-domain [7], [8] and frequency-domain [9], [10].

Conventional multi-channel ANC requires to place the error microphones uniformly distributed inside the control region [11], which is one of the main drawbacks. Space domain signal processing, using harmonics (cylindrical/spherical) based sound field processing, is recently applied in ANC [12], [13] to increase the performance with microphones on the surface of control region. As space domain solution of wave equation is mainly developed in the frequency-domain [14], most of space domain adaptive filter designs are also done in the frequency-domain [11], [12], [15]. Given ANC systems are very sensitive to time latency [16], significant delays from time-frequency transform thus becomes a problem.

Barkefors and Berthilsson [8] has proposed a time-domain multi-channel spatial ANC system, but it requires the error microphones to be distributed uniformly inside the control region, which limits its usage scenario. Work by Zhang et al [11] achieves noise control over a region with error microphones placed on the boundary of the control region. However, this algorithm is designed for a 2D region in frequency-domain. Chen et al [17] achieves noise control for a 3D region in a car. Their approach is also based on

frequency-domain signals, where latency problem introduced by time-frequency transform is still an issue.

In this paper, we first derive a new spherical harmonic based signal decomposition method in time-space domain. Then based on this decomposition method, we propose two new feed-forward adaptive filter designing methods using filtered-x LMS algorithm [16]. These new methods not only have the advantage of space domain signal processing, but also avoid the latency caused by time-frequency domain transform. We compare noise reduction performance of time-domain conventional multi-channel method [16] and our proposed two methods by simulation, finding the proposed methods achieve a higher noise reduction over the control region.

## 2. SYSTEM MODEL

Consider the desired control region as a spherical region of radius  $r$  without any sound sources inside. To measure the residual sound field and to generate secondary sound field, an array of  $Q$  omnidirectional microphones and an array of  $L$  loudspeakers are uniformly placed on the surface of this control region and on a sphere with radius  $R$  ( $R > r$ ), respectively. The aim of this system is to minimize the residual sound field inside the control region by generating a secondary sound field to cancel the primary noise field.

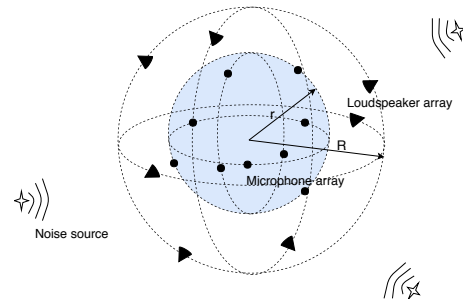


**Fig. 1.** ANC system setup with a spatial control region (shaded area) consisting a microphone array of radius  $r$  and a loudspeaker array of radius  $R$ .

Inside the control region, the residual sound pressure at an arbitrary observation point  $\mathbf{x} = (r_x, \phi_x, \theta_x)$  is influenced by both the noise sources and the loudspeakers. Let  $\mathcal{N}(t)$  be the noise measured by a reference microphone near the noise source at point  $\mathbf{y}_n$ ,  $d_\ell(t)$  be the driving signal of the  $\ell^{\text{th}}$  loudspeaker placed at point  $\mathbf{y}_\ell$ ,  $g(\mathbf{x}|\mathbf{y}_n, t)$  be the propagation function between points  $\mathbf{x}$  and  $\mathbf{y}_n$ . Then, the noise sound field present at  $\mathbf{x}$  can be given by

$$p(\mathbf{x}, t) = \mathcal{N}(t) * g(\mathbf{x}|\mathbf{y}_n, t), \quad (1)$$

This work is supported by Australian Research Council (ARC) grant DP180102375.

where  $*$  denotes convolution operation. Similarly, the secondary sound field generated by the loudspeakers at point  $\mathbf{x}$  is

$$y(\mathbf{x}, t) = \sum_{\ell=1}^L d_{\ell}(t) * g(\mathbf{x}|\mathbf{y}_{\ell}, t). \quad (2)$$

Therefore, the total or residual sound field  $e(\mathbf{x}, t)$  as observed at point  $\mathbf{x}$  is

$$e(\mathbf{x}, t) = p(\mathbf{x}, t) + y(\mathbf{x}, t). \quad (3)$$

In a typical feed-forward adaptive system, the driving signal is obtained by filtering the reference signal  $\mathcal{N}(t)$  using a FIR adaptive filter with an impulse response of  $w_{\ell}(t)$ , i.e.,

$$d_{\ell}(t) = \mathcal{N}(t) * w_{\ell}(t). \quad (4)$$

More details on the process of developing this filter is discussed later in Sec.4. Novelty of this paper lies in the introduction of a time-space domain spherical harmonic decomposition of the wave-field, which facilitates the design of the aforementioned filter characteristics  $w_{\ell}(t)$ .

### 3. TIME-DOMAIN ANALYSIS OF SPHERICAL HARMONIC DECOMPOSITION

Typically, spherical harmonic based signal decomposition is formulated in the frequency-domain. In this section, we develop the corresponding time-domain decomposition method. Note that the time-domain signal decomposition can be used not only for ANC systems, but also other applications involving spatial sound.

Let  $h(\mathbf{x}, t)$  be the sound pressure measured at a point  $\mathbf{x}$  with respect to an origin at time  $t$ , and let  $H(\mathbf{x}, f)$  be the Fourier transform of  $h(\mathbf{x}, t)$ , where  $f$  is the frequency in Hz. Note that  $H(\mathbf{x}, f)$  is a solution to the Helmholtz wave equation [14] and can be expressed as

$$H(\mathbf{x}, f) = \sum_{\nu=0}^{\infty} \sum_{\mu=-\nu}^{\nu} \zeta_{\nu}^{\mu}(f) j_{\nu}\left(\frac{2\pi f r_x}{c}\right) Y_{\nu}^{\mu}(\theta_x, \phi_x), \quad (5)$$

where  $\zeta_{\nu}^{\mu}(k)$  is frequency-dependent spherical harmonic coefficients,  $j_{\nu}(\cdot)$  is the  $n^{\text{th}}$  order spherical Bessel function of the first kind, and  $Y_{\nu}^{\mu}(\cdot)$  are the real valued spherical harmonic function of order  $\nu$  and degree  $\mu$  [18]. For any  $r_x < r$ , we can truncate the infinite summation in (5) at  $V = \lceil kr \rceil$  [19]. Due to the Fourier transform relationship between  $h(\mathbf{x}, t)$  and  $H(\mathbf{x}, f)$ , we can use (5) to write

$$h(\mathbf{x}, t) = \sum_{\nu=0}^V \sum_{\mu=-\nu}^{\nu} \rho_{\nu}^{\mu}(t) * p_{\nu}(t) Y_{\nu}^{\mu}(\theta_x, \phi_x), \quad (6)$$

where  $\rho_{\nu}^{\mu}(t)$  is the inverse Fourier transform of  $\zeta_{\nu}^{\mu}(f)$  and  $p_{\nu}(t)$  is the inverse Fourier transform of  $j_{\nu}(2\pi f r_x/c)$ , which is given by [20]

$$p_{\nu}(t) = \frac{i^{\nu} c}{2r_x} P_{\nu}\left(\frac{tc}{r_x}\right), \quad (7)$$

where  $P_{\nu}(\cdot)$  is the Legendre function of order  $\nu$ . A similar truncation to (5) of order  $V$  can be obtained in (6) since  $\rho_{\nu}^{\mu}(t) * p_{\nu}(t)$  and  $\zeta_{\nu}^{\mu}(k) j_{\nu}(2\pi f r_x/c)$  are Fourier transform pairs.

By integrating (6) over the sphere of radius  $r_x$  and using the orthogonal property of  $Y_{\nu}^{\mu}(\cdot)$ , we derive:

$$\rho_{\nu}^{\mu}(t) * p_{\nu}(t) = \int_0^{2\pi} \int_0^{\pi} h(\mathbf{x}, t) Y_{\nu}^{\mu}(\theta_x, \phi_x) \sin \theta_x d\theta_x d\phi_x. \quad (8)$$

Then, by convolving (8) with  $a_{\nu}(t)$ <sup>1</sup>, where  $a_{\nu}(t) * p_{\nu}(t) = \delta(t)$ , we have

$$\rho_{\nu}^{\mu}(t) = a_{\nu}(t) * \int_0^{2\pi} \int_0^{\pi} h(\mathbf{x}, t) Y_{\nu}^{\mu}(\theta_x, \phi_x) \sin \theta_x d\theta_x d\phi_x. \quad (9)$$

We can approximate the integration in (9) with a finite summation to estimate  $\rho_{\nu}^{\mu}(t)$  [21]. When sound field  $h(\mathbf{x}_q, t)$  is measured for  $q = 1, \dots, Q$  with the error microphones, we can calculate  $\rho_{\nu}^{\mu}(t)$  by

$$\rho_{\nu}^{\mu}(t) \approx a_{\nu}(t) * \sum_{q=1}^Q h(\mathbf{x}_q, t) Y_{\nu}^{\mu}(\theta_q, \phi_q) \Delta_q, \quad (10)$$

where  $\Delta_q$  is a correction factor for approximating an integral by a summation.

## 4. TIME-SPACE DOMAIN ADAPTIVE ALGORITHMS

In this section, we develop two time-space domain feed-forward adaptive methods based on the time-domain Fx-LMS algorithm [16]. We use discrete-time signals and discrete time-space domain coefficients in the following sections, thus the time variable  $t$  is replaced by index  $n$ , where  $t = nT$  and  $T$  is the sampling period.

### 4.1. Formulation of time-space domain signal coefficients

In Sec.3, we introduced the spherical harmonic coefficients of the time-space signal  $h(\mathbf{x}, n)$  as  $\rho_{\nu}^{\mu}(n)$ . By applying this relationship to (3), we have

$$\gamma_{\nu}^{\mu}(n) = \alpha_{\nu}^{\mu}(n) + \beta_{\nu}^{\mu}(n), \quad (11)$$

where  $\gamma_{\nu}^{\mu}(n)$ ,  $\alpha_{\nu}^{\mu}(n)$  and  $\beta_{\nu}^{\mu}(n)$  are the spherical coefficients of  $e(\mathbf{x}, n)$ ,  $p(\mathbf{x}, n)$  and  $y(\mathbf{x}, n)$ , respectively. By substituting for (2) from (4), we have

$$\beta_{\nu}^{\mu}(n) = \sum_{\ell=1}^L \mathcal{N}(n) * T_{\nu, \ell}^{\mu}(n) * w_{\ell}(n), \quad (12)$$

where  $T_{\nu, \ell}^{\mu}(n)$  is the spherical harmonic coefficient of  $g(\mathbf{x}|\mathbf{y}_{\ell}, n)$ .

Based on (11) and (12), we design two time-space domain feed-forward adaptive filters in the following sections with the block diagram shown in Fig. 2. By deriving the adaptive update algorithm

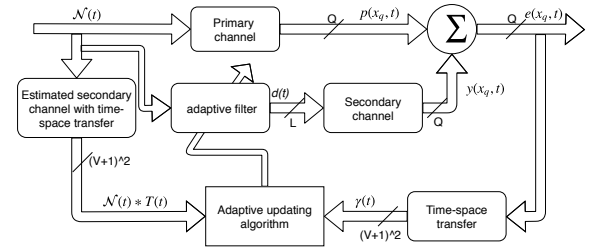


**Fig. 2.** Block diagram of time-space domain adaptive algorithms.

of  $w_{\ell}(n)$ , we aim to minimize  $\gamma_{\nu}^{\mu}(n)$ , which represents the residual sound field  $e(\mathbf{x}, n)$  over the control region.

<sup>1</sup>Note that  $a_{\nu}(t)$  can be constructed by taking the inverse Fourier transform of  $1/j_{\nu}(2\pi f r/c)$  and using a suitable band stop filter to avoid Bessel zeros.

## 4.2. Minimizing Squared Residual Sound Field Coefficient Error over Region (MSE-R)

Let  $\mathbf{W} = [\mathbf{w}_1, \mathbf{w}_2, \mathbf{w}_3, \dots, \mathbf{w}_L]$ , where  $\mathbf{w}_\ell$  is the vector of filter taps for the  $\ell^{\text{th}}$  loudspeaker, with order of  $L_w$ . To minimize the residual sound field, we define the adaptive algorithm cost function as

$$\xi(n) = \sum_{\nu=0}^V \sum_{\mu=-\nu}^{\nu} \|\gamma_{\nu}^{\mu}(n)\|^2. \quad (13)$$

Taking the derivative of  $\xi$  with respect to  $\mathbf{W}(n)$ , and by using (11) and (12), we derive

$$\begin{aligned} \nabla \xi(n) &= \frac{\partial \xi(n)}{\partial \mathbf{W}(n)} = \sum_{\nu=0}^V \sum_{\mu=-\nu}^{\nu} 2\gamma_{\nu}^{\mu}(n) \left[ \frac{\partial \gamma_{\nu}^{\mu}(n)}{\partial \mathbf{W}(n)} \right] \\ &= 2 \sum_{\nu=0}^V \sum_{\mu=-\nu}^{\nu} \gamma_{\nu}^{\mu}(n) \mathbf{S}_{\nu}^{\mu}(n), \end{aligned} \quad (14)$$

where  $\mathbf{S}_{\nu}^{\mu}(n)$  is a matrix of size of  $L \times L_w$  with its  $\ell^{\text{th}}$  column and  $\tau^{\text{th}}$  row element at time-index  $n$  given by

$$s_{\nu}^{\mu}(\ell, \tau) = \mathcal{N}(n - \tau) * T_{\nu, \ell}^{\mu}(n), \quad (15)$$

where  $\mathcal{N}(n - \tau)$  is  $\mathcal{N}(n)$  delayed by  $\tau$  samples. For conventional multi-channel adaptive filters, the update equation is typically given by [16]

$$\mathbf{W}(n+1) = \mathbf{W}(n) - \frac{\lambda}{2} \nabla \xi(n), \quad (16)$$

where  $\lambda$  is the step size. Hence, for each secondary loudspeaker, the  $\tau^{\text{th}}$  element of time-space domain update equation is

$$\begin{aligned} \mathbf{w}_{\ell, \tau}(n+1) &= \mathbf{w}_{\ell, \tau}(n) - \lambda \sum_{\nu=0}^V \sum_{\mu=-\nu}^{\nu} \gamma_{\nu}^{\mu}(n) \\ &\quad \times [\mathbf{N}(n - \tau)^T * T_{\nu, \ell}^{\mu}(n)]. \end{aligned} \quad (17)$$

We implement our adaptive algorithm (17) by the following steps: a) pre-estimate the impulse response of secondary channel  $g(\mathbf{x}_q | \mathbf{y}_\ell, n)$  from each loudspeaker to each microphone, b) measure the error signal  $e(\mathbf{x}_q, n)$  by error microphones, and reference signal  $\mathcal{N}(n)$  by the reference microphone, c) estimate  $\gamma_{\nu}^{\mu}(n)$  and  $T_{\nu, \ell}^{\mu}(n)$ .

To obtain  $\gamma_{\nu}^{\mu}(n)$  and  $T_{\nu, \ell}^{\mu}(n)$  using (10), an inverse Fourier transform based function  $a_{\nu}(n)$  is involved, where its group delay can lower performance and slow down convergence and its Bessel zeros can influence stability, which are not desirable in the system. Therefore, in the next section, we study an alternate cost function to avoid these drawbacks.

## 4.3. Minimizing Squared Residual Sound Field Error on the Region Boundary (MSE-B)

Instead of minimizing the residual sound field over the whole control region as in Sec. 4.2, here we only minimize the residual sound field on the boundary. As there are no noise sources inside the region, this method should still achieve an acceptable noise reduction within the region.

We define the adaptive algorithm cost function as

$$\xi = \sum_{\nu=0}^V \sum_{\mu=-\nu}^{\nu} \|\eta_{\nu}^{\mu}(n)\|^2, \quad (18)$$

where

$$\begin{aligned} \eta_{\nu}^{\mu}(n) &= \gamma_{\nu}^{\mu}(n) * p_{\nu}(n) \\ &= \int_0^{2\pi} \int_0^{\pi} e(\mathbf{x}, t) Y_{\nu}^{\mu}(\theta_x, \phi_x) \sin \theta_x d\theta_x d\phi_x \\ &\approx \sum_{q=1}^Q e(\mathbf{x}_q, n) Y_{\nu}^{\mu}(\theta_q, \phi_q) \Delta q. \end{aligned} \quad (19)$$

By taking the derivative of  $\xi$  in (18) with respect to  $\mathbf{W}(n)$  and using (11) and (12), the gradient of this cost function can be derived as

$$\begin{aligned} \nabla \xi &= \frac{\partial \xi}{\partial \mathbf{W}(n)} = \sum_{\nu=0}^V \sum_{\mu=-\nu}^{\nu} 2\eta_{\nu}^{\mu}(n) \left[ \frac{\partial \eta_{\nu}^{\mu}(n)}{\partial \mathbf{W}(n)} \right] \\ &= 2\eta_{\nu}^{\mu}(n) [\mathbf{S}_{\nu}^{\mu}(n) * p_{\nu}(n)]. \end{aligned} \quad (20)$$

With (16) and (20), for each loudspeaker, the  $\tau^{\text{th}}$  element of the update equation is

$$\begin{aligned} \mathbf{w}_{\ell, \tau}(n+1) &= \mathbf{w}_{\ell, \tau}(n) - \lambda \sum_{\nu=0}^V \sum_{\mu=-\nu}^{\nu} [\gamma_{\nu}^{\mu}(n) * p_{\nu}(n)] \\ &\quad \times \{ [\mathbf{N}(n - \tau)^T * T_{\nu, \ell}^{\mu}(n)] * p_{\nu}(n) \} \\ &= \mathbf{w}_{\ell, \tau}(n) - \lambda \sum_{\nu=0}^V \sum_{\mu=-\nu}^{\nu} \sum_{q=1}^Q e(\mathbf{x}_q, n) Y_{\nu}^{\mu}(\theta_q, \phi_q) \\ &\quad \times [\mathbf{N}(n - \tau)^T * \sum_{q=1}^Q G(\mathbf{x}_q | \mathbf{y}_\ell, n) Y_{\nu}^{\mu}(\theta_q, \phi_q)]. \end{aligned} \quad (21)$$

In this case, we avoid calculating  $a_{\nu}(n)$  to obtain the update equation, hence avoid latency of inverse Fourier transform and Bessel zeros problem.

## 5. SIMULATION RESULTS AND ANALYSIS

In this section, we compare the performances of the proposed methods (MSE-R, MSE-B) against the conventional multi-channel adaptive filtering method (MP) [22] in both free space and room environment.

We simulate a feed-forward ANC system consisting 9 error microphones and 9 loudspeakers uniformly spaced on two concentric spheres of radius 0.16 m and 0.48 m [23], respectively. A single noise source is located at  $(2, 90^\circ, 90^\circ)$ , where a reference microphone is placed nearby to obtain reference signals. We consider four different noise signals in this simulation, each lasting 1 s.

**Scenario 1:** Multiple superimposing sine wave of frequency 100 Hz, 170 Hz, and 250 Hz;

**Scenario 2:** Single sine wave of frequency 210 Hz;

**Scenario 3:** filtered Gaussian distributed random signal with a 600 Hz cut-off low-pass filter;

**Scenario 4:** filtered real noise recorded in a computer room with a 600 Hz cut-off low-pass filter.

A signal-to-noise ratio (SNR) of 60 dB is added to the microphone recordings for the first three scenarios. Sampling rate is 48 kHz, yet we down sampled at a rate of 10 to reduce computational cost. In order to simulate the reverberant room environment, the image-source method [24] is employed, where the room size is set to be 4 m  $\times$  5 m  $\times$  3 m with reflection coefficients of 0.9, 0.7, 0.8, 0.6, 0.5 and 0.8 of 4 walls and floor and roof respectively.

We define a metric for noise reduction at point  $\mathbf{x}$  inside the control region as

$$\varepsilon(\mathbf{x}) = 10 \log_{10} \frac{\sum_n e(\mathbf{x}, n)^2}{\sum_n p(\mathbf{x}, n)^2}, \quad (22)$$

where the summation is over the last 480 samples of the signals.

We first plot the performance of scenario 1 on the x-y plane with red and blue circles indicating the sphere where the error microphones and the loudspeakers are located, respectively.

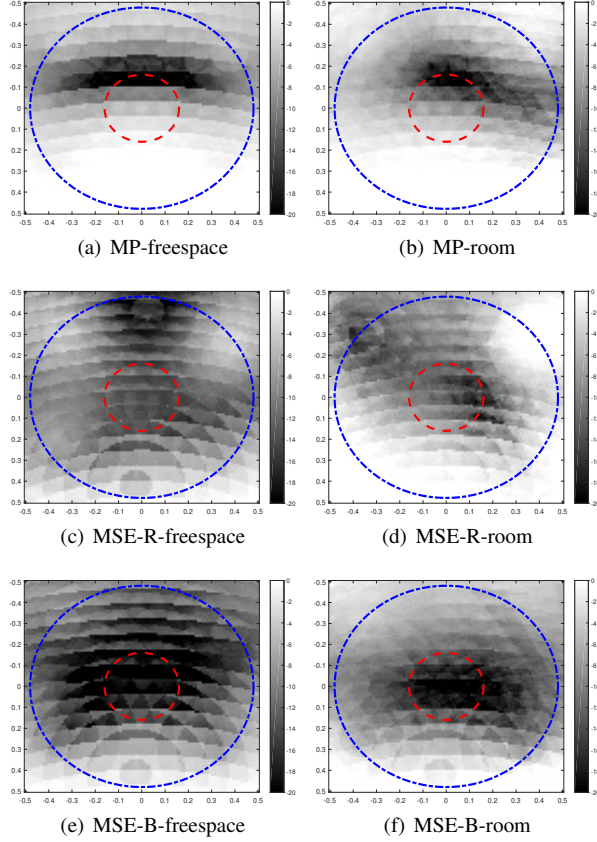


**Fig. 3.** Noise reduction performance in free field with a) MP, c) MSE-R, e) MSE-B, and in a reverberant room with b) MP, d) MSE-R, f) MSE-B.

As shown in Fig.3, all methods can achieve some level of noise reduction in both free-space and room environment. However, it is clearly observed that the noise reduction within the entire control region is better with the proposed methods while MSE-B method achieves the highest performance. With MSE-B method, we can see that almost every test point inside the control region is dark, which refers to around 20 dB noise reduction.

Performance of these methods over the whole region are theoretically evaluated by averaging  $\varepsilon(\mathbf{x})$  over the whole control region with 2103 uniformly placed points.

**Table 1.** Average performance over the whole region in free-space.

	MP	MSE-R	MSE-B
Single sine wave	5.55	18.76	21.27
Multi sine wave	6.52	14.06	20.92
Random noise	16.11	16.85	21.85
Real noise	9.00	10.03	13.50

Table 1 shows the results of average performance over the whole region for four scenarios and three different methods in free space. From Table 1, we note that the proposed two methods achieve higher performance than MP method. MSE-B method achieves the highest noise reduction with all scenarios. For stationary signals, MSE-R method performs significantly better than MP method.

Table 2 shows the results of average performance over the whole region for the four scenarios mentioned earlier and three different methods in room environment. We find the same trends as in free-

**Table 2.** Average performance over the whole region in room.

	MP	MSE-R	MSE-B
Single sine wave	8.60	20.09	23.67
Multi sine wave	8.85	13.43	17.51
Random noise	5.56	10.83	9.56
Real noise	4.40	5.72	4.41

space with sinusoidal noises, that MSE-B method achieves the highest performance. When the noise signals are non-stationary, MSE-R method achieves the highest performance, which is different from what we found in free space.

Theoretically, MSE-R method should achieve the highest performance since it minimizes the coefficients over the whole control region. However, we note the different results in free space and for stationary signals in room from the simulation. This phenomenon is due to the group delay as described in Sec.4.2. In free space, the system delay is mainly caused by filtering methods, hence we obtain an obvious difference on performance between MSE-R method and MSE-B method. Using an advanced windowing method can help to decrease the delay [25].

However in the room environment, as the reverberation from walls makes the impulse responses between loudspeakers and microphones longer, the latency of the whole system becomes much more longer than in free-space. Non-stationary noises have time-varying frequency responses, hence are more sensitive with the delays. We can observe in the room environment, performance of non-stationary signals with all three methods are smaller than stationary signals. With those non-stationary noises, as the delays caused by filtering methods are much more shorter than channel delays in the room, MSE-R achieves the best performance with its strong control over the whole control region.

## 6. CONCLUSION

In this paper, we first derive a spherical harmonic based time-space domain signal decomposition method, providing a novel tool for spatial sound field analysis without transforming signals to frequency-domain. Based on that, we proposed two time-space domain methods for feed-forward adaptive filtering to achieve noise reduction over a spherical region. We compared the noise reduction performance of these proposed methods against conventional time-domain multi-channel ANC system in both free-space and reverberant room environments, finding that the proposed two methods perform better with both narrow-band noise and wide-band noise signals. In simple environment like free-space, MSE-B method achieved the best performance because of its short filtering latency. In reverberant rooms with long and complex channels between microphones and loudspeakers, MSE-R method achieved the best performance with non-stationary noises since it minimizes the coefficients of residual signals over the whole control region.

## 7. REFERENCES

- [1] C. C. Fuller, S. Elliott, and P. A. Nelson, *Active control of vibration*, Academic Press, 1996.
- [2] Y. Kajikawa, W. S. Gan, and S. M. Kuo, "Recent advances on active noise control: open issues and innovative applications," *APSIPA Transactions on Signal and Information Processing*, vol. 1, pp. 21, Aug. 2012.
- [3] J. Zhang, T. D. Abhayapala, P. N. Samarasinghe, W. Zhang, and S. Jiang, "Multichannel active noise control for spatially sparse noise fields," *The Journal of the Acoustical Society of America*, vol. 140, no. 6, pp. 510–516, 2016.
- [4] H. Sano, T. Inoue, A. Takahashi, K. Terai, and Y. Nakamura, "Active control system for low-frequency road noise combined with an audio system," *IEEE Transactions on speech and audio processing*, vol. 9, no. 7, pp. 755–763, 2001.
- [5] P. N. Samarasinghe, W. Zhang, and T. D. Abhayapala, "Recent advances in active noise control inside automobile cabins: Toward quieter cars," *IEEE Signal Processing Magazine*, vol. 33, no. 6, pp. 61–73, 2016.
- [6] A. Montazeri and C. J. Taylor, "Modeling and analysis of secondary sources coupling for active sound field reduction in confined spaces," *Mechanical Systems and Signal Processing*, vol. 95, pp. 286–309, Oct. 2017.
- [7] M. Bouchard and S. Quednau, "Multichannel recursive-least-square algorithms and fast-transversal-filter algorithms for active noise control and sound reproduction systems," *IEEE Transactions on Speech and Audio Processing*, vol. 8, no. 5, pp. 606–618, 2000.
- [8] A. Barkefors, S. Berthilsson, and M. Sternad, "Extending the area silenced by active noise control using multiple loudspeakers," in *Proc. IEEE International Conference on Acoustics, Speech and Signal (ICASSP)*, Mar. 2012, pp. 325–328.
- [9] B. Rafaely and S. J. Elliott, "An adaptive and robust feedback controller for active control of sound and vibration," *Proc. UKACC International Conference on Control*, pp. 1149–1153, 1996.
- [10] J. Benesty and D. R. Morgan, "Frequency-domain adaptive filtering revisited, generalization to the multi-channel case, and application to acoustic echo cancellation," in *Proc. IEEE International Conference on Acoustics, Speech, and Signal Processing*, 2000, vol. 2, pp. 789–792.
- [11] J. Zhang, T. D. Abhayapala, W. Zhang, P. N. Samarasinghe, and S. Jiang, "Active noise control over space: A wave domain approach," *IEEE/ACM Transactions on Audio, Speech and Language Processing (TASLP)*, vol. 26, no. 4, pp. 774–786, 2018.
- [12] P. Peretti, S. Cecchi, L. Palestini, and F. Piazza, "A novel approach to active noise control based on wave domain adaptive filtering," in *Proc. IEEE Workshop on Applications of Signal Processing to Audio and Acoustics*, Oct. 2007, pp. 307–310.
- [13] J. Zhang, T. D. Abhayapala, P. N. Samarasinghe, W. Zhang, and S. Jiang, "Sparse complex fxlms for active noise cancellation over spatial regions," in *Proc. IEEE International Conference on Acoustics, Speech and Signal Processing (ICASSP)*, Mar. 2016, pp. 524–528.
- [14] E. G. Williams, *Fourier acoustics: sound radiation and nearfield acoustical holography*, Elsevier, 1999.
- [15] S. Spors and H. Buchner, "An approach to massive multichannel broadband feedforward active noise control using wave-domain adaptive filtering," in *Proc. IEEE Workshop on Applications of Signal Processing to Audio and Acoustics*, Oct. 2007, pp. 171–174.
- [16] S. M. Kuo and D. R. Morgan, *Active noise control systems: algorithms and DSP implementations*, John Wiley & Sons, Inc., 1995.
- [17] H. Chen, P. Samarasinghe, T. D. Abhayapala, and W. Zhang, "Spatial noise cancellation inside cars: Performance analysis and experimental results," in *Proc. IEEE Workshop on Applications of Signal Processing to Audio and Acoustics (WASPAA)*, Oct. 2015, pp. 1–5.
- [18] H. H. H. Homeier and E. O. Steinborn, "Some properties of the coupling coefficients of real spherical harmonics and their relation to gaunt coefficients," *Journal of Molecular Structure: THEOCHEM*, vol. 368, pp. 31–37, Sep. 1996.
- [19] D. B. Ward and T. D. Abhayapala, "Reproduction of a plane-wave sound field using an array of loudspeakers," *IEEE Transactions on speech and audio processing*, vol. 9, no. 6, pp. 697–707, 2001.
- [20] M. Abramowitz and I. A. Stegun, *Handbook of mathematical functions: with formulas, graphs, and mathematical tables*, vol. 55, Courier Corporation, 1965.
- [21] T. D. Abhayapala, D. B. Ward, et al., "Theory and design of high order sound field microphones using spherical microphone array," in *Proc. IEEE International Conference on Acoustics, Speech, and Signal Processing*, 2002, vol. 2, pp. 1949–1952.
- [22] S. M. Kuo and D. R. Morgan, "Active noise control: a tutorial review," *Proceedings of the IEEE*, vol. 87, no. 6, pp. 943–973, 1999.
- [23] N. J. A. Sloane, R. H. Hardin, W. D. Smith, et al., "Tables of spherical codes," See <http://www.research.att.com/njas/-packings>, 2000.
- [24] J. B. Allen and D. A. Berkley, "Image method for efficiently simulating small-room acoustics," *The Journal of the Acoustical Society of America*, vol. 65, no. 4, pp. 943–950, 1979.
- [25] F. Zhang, Z. Geng, and W. Yuan, "The algorithm of interpolating windowed fft for harmonic analysis of electric power system," *IEEE transactions on power delivery*, vol. 16, no. 2, pp. 160–164, 2001.